

FIRST MEASUREMENT OF THE LEFT-RIGHT CROSS SECTION ASYMMETRY IN Z BOSON PRODUCTION AT $E_{CM} = 91.55$ GEV

The SLD Collaboration[◊]
 presented by P.C. Rowson

Columbia University, Department of Physics, New York, NY 10027
 Stanford Linear Accelerator Center, Stanford University, Stanford, CA 94309

Abstract

The left-right cross section asymmetry for Z boson production in e^+e^- annihilation (A_{LR}) has been measured at $E_{cm} = 91.55$ GeV with the SLD detector at the SLAC Linear Collider (SLC) using a longitudinally polarized electron beam. The electron polarization was continually monitored with a Compton scattering polarimeter, and was typically 22 %. We have accumulated a sample of $\sim 10,200$ Z events. We find that $A_{LR} = 0.100 \pm 0.044 \pm 0.003$ where the first error is statistical and the second is systematic. From this measurement, we determine the weak mixing angle defined at the Z boson pole to be $\sin^2 \theta_W^{\text{lept}} = 0.2378 \pm 0.0056$.

INTRODUCTION

This paper presents the result of a measurement of the left-right cross section asymmetry (A_{LR}) in the production of Z bosons by e^+e^- collisions performed by the SLD Collaboration at the SLAC Linear Collider.¹

The left-right asymmetry is defined as follows,

$$A_{LR} \equiv \frac{\sigma(e^+e_L^- \rightarrow Z) - \sigma(e^+e_R^- \rightarrow Z)}{\sigma(e^+e_L^- \rightarrow Z) + \sigma(e^+e_R^- \rightarrow Z)}, \quad (1)$$

where $\sigma(e^+e_L^- \rightarrow Z)$ and $\sigma(e^+e_R^- \rightarrow Z)$ are the production cross sections for Z bosons with left-handed and right-handed electrons, respectively. Within the context of the Standard Model, this quantity is a sensitive function of the electroweak mixing parameter $\sin^2 \theta_W^{\text{lept}}$,

$$A_{LR} = \frac{2v_e a_e}{v_e^2 + a_e^2} = \frac{2 \left[1 - 4 \sin^2 \theta_W^{\text{lept}} \right]}{1 + \left[1 - 4 \sin^2 \theta_W^{\text{lept}} \right]^2}, \quad (2)$$

where v_e and a_e are the vector and axial vector coupling constants of the Z boson to the elec-

tron current. Note that A_{LR} is sensitive to the initial state couplings and is insensitive to the final state couplings.³ The left-right asymmetry has the following properties:³ it is sensitive to virtual electroweak corrections; it is insensitive to real radiative corrections; it is a weak function of center-of-mass energy, E_{cm} , near the Z pole; and it is expected to be relatively large, in the range 0.10-0.15.

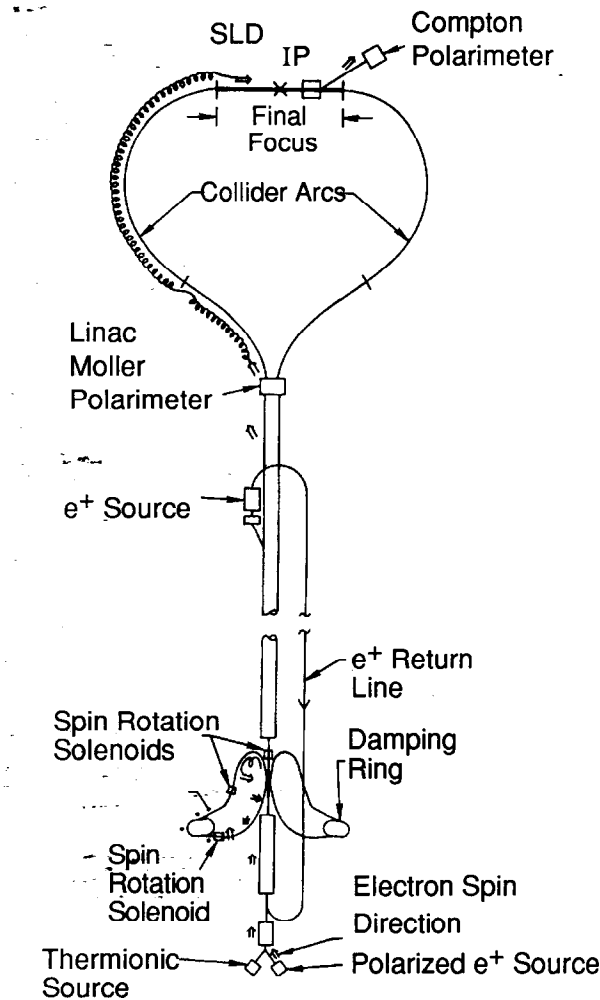
We measured A_{LR} by counting all hadronic decay modes of the Z boson (the sample also contains $\tau^+\tau^-$ final states) for each of the two longitudinal polarization states of the electron beam. The measurement does not require an absolute luminosity measurement or any knowledge of the absolute detector acceptance and efficiency.⁴

THE POLARIZED ELECTRON BEAM AT THE SLC

The SLAC Linear Collider (SLC) was designed to produce, accelerate, and collide a spin-polarized electron beam.⁵ A diagram of the SLC is shown in Figure 1. The polarized electron source consists of a GaAs photocathode that is illuminated by a circularly polarized laser beam.⁶ The emitted electrons

^{*}Work supported by Department of Energy contract DE-AC03-76SF00515.

[◊]List of authors follows the list of references.



POLARIZATION IN THE OVERALL SLC LAYOUT

9-92

7220A1

Figure. 1. The SLC. The electron spin direction is indicated by the double-arrow.

are longitudinally polarized, and the electron helicity is changed randomly on a cycle-by-cycle basis (the SLC operates at 120 Hz). The polarization of the emitted electrons is typically 28 %.

A system composed of the dipole magnets in the transfer line from the linac to the damping rings, and a superconducting solenoid magnet, is used to rotate the longitudinal polarization of the beam into the vertical direction to preserve polarization during storage in the damping ring. A system composed of two superconducting solenoids and the dipole magnets in the return line to the linac is used to reorient the polarization vector

upon extraction from the damping ring. This system has the ability to provide nearly all polarization orientations in the linac. A fractional polarization loss of 5 % occurs in the damping ring.

The electron pulse is transported through the North Arc and Final Focus systems of the SLC to the interaction point (IP) of the machine. Polarization loss in the arcs due to energy dispersion is expected to be 5-10 fractionally, while the net spin rotation due to the arc system is sensitive to the parameters of the orbit and is measured empirically. The spin rotation system is adjusted to maximize the longitudinal polarization at the IP.

After passing through the interaction point, the longitudinal component of the electron beam polarization is measured with a Compton polarimeter. The Compton polarimeter, which will be described in the next section, measured a typical IP polarization of 22 %.

The electron and positron beams are then transported to the south and north beam dumps, respectively, where precision energy spectrometers⁷ are located upstream of the beam dumps and monitor the beam energies continually. The mean electron and positron energies were measured to be 45.71 GeV and 45.84 GeV, respectively. The mean center-of-mass energy was $E_{cm} = 91.55 \pm 0.04$ GeV.

THE POLARIZATION MEASUREMENT

The Compton polarimeter continually monitors the longitudinal polarization of the electron beam after it has passed through the IP and before it is deflected by dipole magnets. Polarimeter data are acquired continually for intervals of 20,000 SLC cycles (~3 min) and are logged in summary form onto SLD data tapes. A diagram of the polarimeter is shown in Figure 2. The electron beam collides with a circularly polarized photon beam which is produced by a frequency-doubled Nd:YAG laser of wavelength 532 nm. The scattered and unscattered beams remain unseparated until they pass through a pair of dipole magnets.

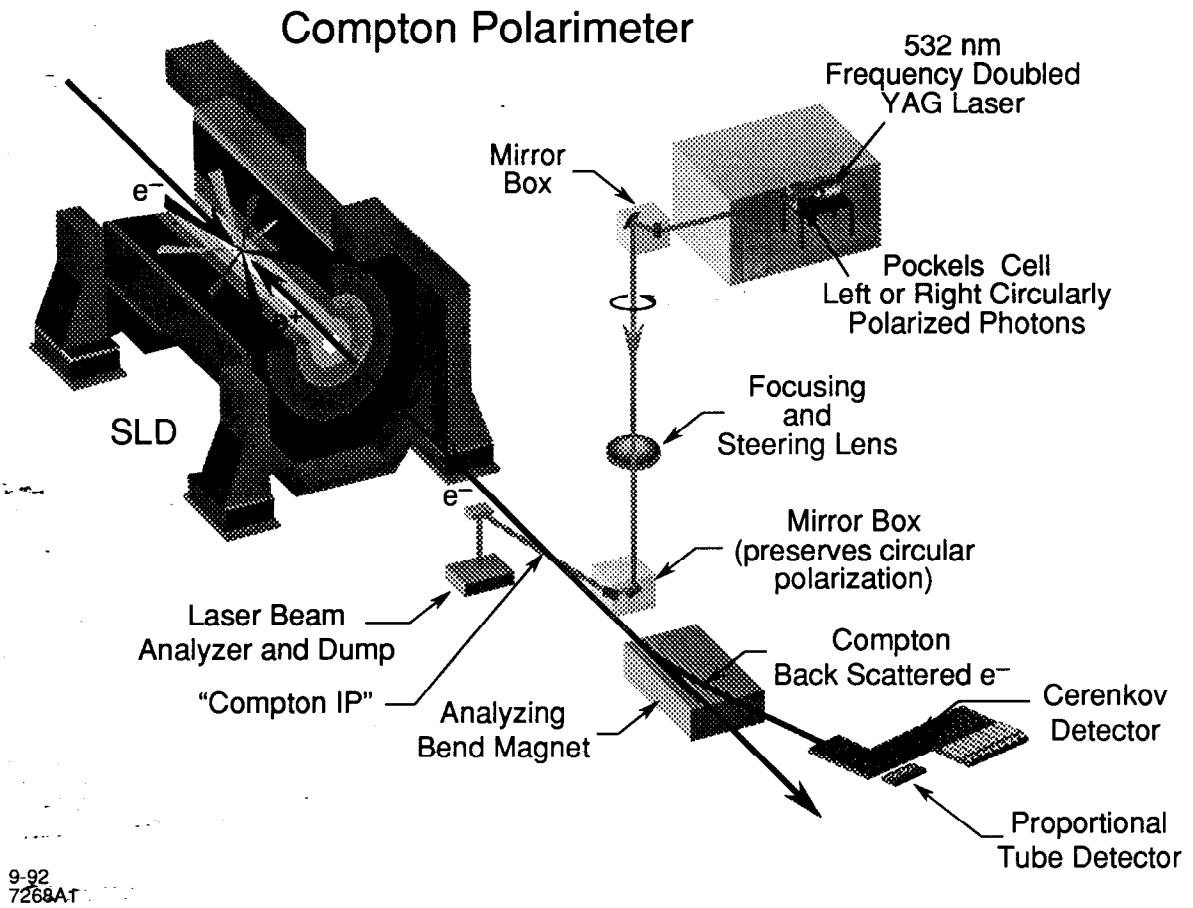


Figure 2. A schematic diagram of the Compton Polarimeter.

The scattered electrons are dispersed horizontally and exit the vacuum system through a thin window. Electrons in the energy interval 15-30 GeV are detected and momentum analyzed by a pair of redundant multichannel detectors (a Cherenkov detector and a proportional tube detector). We measure the counting rates in the detectors for anti-parallel and parallel photon/electron beam helicities; given the laser polarization the asymmetry formed from these rates determines the electron beam polarization.⁸ The circular polarization of the laser beam at the Compton IP was measured to be $93 \pm 2\%$. The absolute helicity of the laser polarization was determined from comparison with a calibrated quarter-wave plate.⁹ In order to avoid systematic effects, the sign of the circular polarization is changed randomly on sequential laser pulses.

The channel-by-channel polarization asymmetry as measured by the Cherenkov detector is shown in Figure 3. The solid histogram represents the best fit of the data to a convolution of the theoretical asymmetry and a simulated response function of the spectrometer. The errors reflect the systematic uncertainties in the transverse position of the detector and the momentum scale of the spectrometer, which are determined from measurements of the minimum electron energy point and the zero-asymmetry point.

Including effects due to the Compton polarimeter spectrometer and laser systems, we estimate the total relative systematic error on the polarization ($\frac{\delta P}{P}$) to be 3%.

We have performed a number of checks of the polarization measurement. The polarimeter measures the electron scattering rate for two helicity states of electrons and two helicity states of photons. From these rates we

THE SLD DETECTOR AND EVENT SELECTION

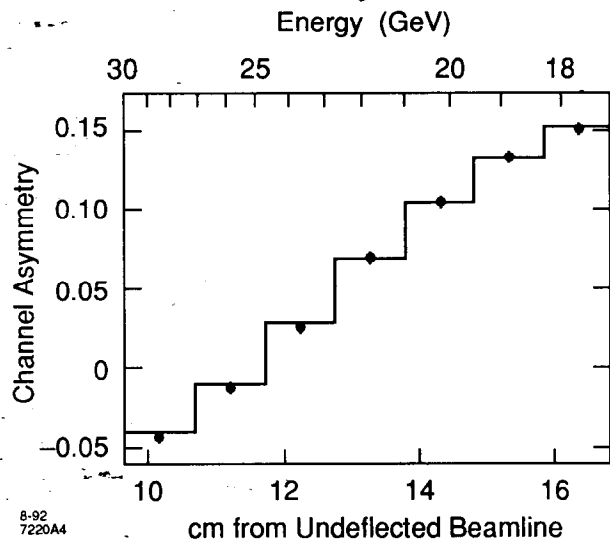


Figure 3. The polarization asymmetry measured by seven channels of the Cerenkov detector. The solid histogram represents the best fit of the data to a convolution of the theoretical asymmetry and a simulated response function of the spectrometer.

form two non-zero asymmetries and two null asymmetries, and we verify that the nonzero asymmetries are consistent and that the null asymmetries are consistent with zero.

An additional systematic error would arise if the average beam polarization at the Compton interaction point differed from the luminosity-weighted average beam polarization at the SLC interaction point (the true polarization). We have investigated a number of possible effects, none of which exceeds the level of a relative 0.1%. For example, the SLC collision point and the electron-photon collision point are separated by a lattice of quadrupole magnets. The beam divergence is different at the two points and the beam direction could be different at the two points. We estimate that these effects cause the measured and true polarizations to differ by less than a relative 0.07%. For details on other effects, see references.^{10,11}

The polarized e^+e^- collisions are measured by the SLD detector which has been described elsewhere.¹² This analysis makes use of the liquid argon (LAC)¹³ and warm iron (WIC)¹⁴ calorimeter systems to measure the energies of final state particles, the central drift chamber (CDC) to reconstruct the trajectories of charged particles in a solenoidal magnetic field of 0.6 T, and the luminosity monitoring system (LUM)¹⁵ to measure the rate of small-angle Bhabha scattering events.

The sample of Z decays used here was selected via a calorimetric analysis based largely upon the LAC. The calorimetric analysis must distinguish Z events from several backgrounds that are unique to the operation of a linear collider and differ from those encountered at e^+e^- storage rings. The backgrounds fall into two major categories: those due to low energy electrons and photons that scatter from various beamline elements and apertures, and those due to high energy muons that traverse the detector parallel to the beam axis (due to the low average current in the SLC, backgrounds caused by beam collisions with residual gas in the beamline are negligible). We make use of the fine segmentation and tower geometry of the LAC to suppress both backgrounds. All electromagnetic and hadronic LAC towers used in the analysis are required to satisfy a combination of tower threshold cuts and criteria that select against radially isolated energy deposition in a combined electromagnetic-hadronic tower. All events are required to satisfy a set of global event cuts based on total visible energy and energy balance.

Our Z events are associated with polarization measurements by proximity in time, where we require that all acceptable events must have been recorded by the SLD detector within 1 hour of a polarization measurement.

As we describe in the next section, a control sample is provided by small-angle Bhabha

scattering events selected using the LUM system. The accepted Bhabha scattering cross section is approximately twice the total cross section for hadronic Z final states.

The sign of the electron beam helicity is supplied to the SLD data acquisition system via two redundant data paths. The correct synchronization of the helicity signals with triggered and logged events is verified by the following procedure: The positron beam is turned off. The electron source is modified to deliver beam for only one of the two electron helicity states. Data are logged with a low threshold LAC trigger or a random trigger. An offline analysis is then used to verify that radiation is observed in the various detector subsystems only for events of the expected helicity. This test has been performed on seven occasions to date. During the tests, the rate of improperly synchronized pulses was less than 0.05% at 95% confidence.

We estimate that the combined efficiency of the trigger and the Z selection criteria is about 92% for hadronic Z decays. Comparing this selection procedure with one that is based upon tracking information¹⁶ and by applying our selection procedure to Monte Carlo events, we estimate that the residual beam-related background in the Z sample is less than 1%. The contribution of two-photon processes to the Z sample has been estimated by a Monte Carlo simulation to be less than 0.1%. Another component of our sample, tau lepton pairs, constitute an estimated $1.5 \pm 0.5\%$ of the sample. Since tau pair events manifest the correct value of A_{LR} , we do not remove them from the sample. Final state e^+e^- events are removed since the presence of the t-channel photon exchange subprocess dilutes the value of A_{LR} . We apply an e^+e^- identification procedure which searches for large and highly localized energy deposition in the electromagnetic section of the LAC. The residual e^+e^- background in the hadronic Z sample is about 0.5%.

A total of 10,224 Z events and 25,615 small-angle Bhabha events satisfy the selection criteria. We find that 5,226 of the Z events and 12,832 of the small-angle Bhabha events were produced with left-handed electron beam and 4,998 of the Z events and 12,783 of the Bhabha events were produced with right-handed beam.¹⁷

DETERMINATION OF A_{LR}

The left-right asymmetry is defined in equation (1) in terms of the cross sections for completely polarized electron beams colliding with an unpolarized positron beam. For the case where luminosity, event detection efficiency, electron polarization and backgrounds are helicity-independent (and we will justify these assumptions), the following simple expression holds :

$$A_{LR} = \frac{A_{meas}}{\mathcal{P}} = \frac{1}{\mathcal{P}} \cdot \left(\frac{N_L - N_R}{N_L + N_R} \right), \quad (3)$$

where A_{meas} is the observed asymmetry, \mathcal{P} is the luminosity-weighted, average polarization and N_L and N_R are the total event counts produced by left- and right-handed electron beam respectively.

The helicity dependence of event acceptance is negligibly small.⁴ The Compton polarimeter measures the difference between left- and right-handed beam polarization to be less than 5×10^{-3} . There is considerable reason to believe that the left-right SLC luminosity asymmetry is also quite small. The use of a Pockels cell to reverse the source laser helicity provides a very powerful constraint upon possible differences in the left-handed and right-handed electron beams produced by the photoemission gun. In addition, since the couplings of the electron spins to fields of the beam transport system are much weaker than the corresponding couplings of the electron charges, we expect that the beams remain nearly identical as they are damped, accelerated, and transported to the interaction point. Finally, the use of random sign reversal of

the electron beam helicity insures that there are no correlations between the beam helicity and periodic variations in the SLC luminosity.

In order to investigate a possible left-right luminosity difference, we have compared a number of electron beam parameters by helicity. We verify that the beam currents, energies, and energy spreads are independent of the beam helicity. The beam position and direction at the end of the linac are also independent of helicity. We verify that the flux of beamstrahlung photons produced by beam-beam interactions is independent of the beam helicity.¹⁸ From these checks we conservatively estimate that the left-right SLC luminosity asymmetry is less than 10^{-3} . We have also checked that the numbers of left-handed and right-handed pulses logged by the SLD data acquisition system are equal to within statistical errors.

Finally, we note that the left-right asymmetry of the small-angle Bhabha scattering cross section is expected to be very small ($\sim 10^{-4}$). Therefore, the numbers of small-angle Bhabha events produced from left-handed and right-handed beams, N_{lumL} and N_{lumR} respectively, measure the relative left-handed and right-handed luminosities. The relative luminosities may be expressed in terms of the luminosity asymmetry, $A_{lum} \equiv (N_{lumL} - N_{lumR}) / (N_{lumL} + N_{lumR})$, which we currently measure to be $A_{lum} = 0.002 \pm 0.006$.

The average polarization can be estimated from measurements of the beam polarization that are made when valid Z events are recorded,

$$\mathcal{P} \equiv \frac{1}{N_Z} \sum_{i=1}^{N_Z} \mathcal{P}_i, \quad (4)$$

where N_Z is the total number of Z events, and \mathcal{P}_i is the polarization that was measured when the i^{th} event was logged. We evaluate the luminosity-weighted polarization to be

$$\mathcal{P} = 22.4 \pm 0.7\%,$$

where the error is dominated by the systematic uncertainty on the polarimeter measurements.

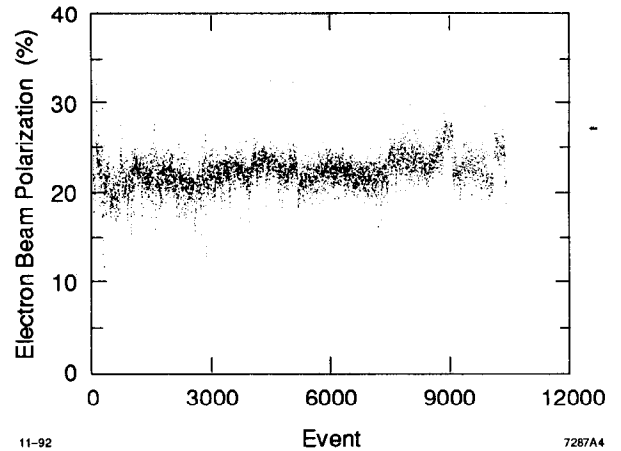


Figure 4. The electron beam polarization as sampled when each Z event was logged.

Using equation (3), we find the left-right asymmetry to be

$$A_{LR} = 0.100 \pm 0.044(\text{stat.}) \pm 0.003(\text{sys.}).$$

The systematic error is dominated by the error on the polarization determination.

CONCLUSIONS AND PLANS

We report a measurement of the left-right asymmetry in the Z boson production cross section at $E_{cm} = 91.55$ GeV. Using a sample of 10,224 hadronic events, we find the left-right asymmetry to be $0.100 \pm 0.044 \pm 0.003$. We calculate the electroweak mixing parameter to be

$$\sin^2 \theta_W^{\text{lept}} = 0.2378 \pm 0.0056(\text{stat.} + \text{sys.}),$$

where we have corrected the result to account for the deviation of the SLC center-of-mass energy from the Z -pole energy and for initial state radiation (the correction from the result given by equation (2) is $+0.0003$)¹⁹. Our result is consistent with recent results from the LEP experiments.²⁰

In the future, we expect to make a number of improvements. We anticipate significant improvements in SLC luminosity, leading to an accumulated data sample of more than 50,000 events during the upcoming 1993 run. We expect to increase the electron polarization to a

value above 40%. It may be possible to make use of the recent development of strained lattice cathodes²¹ to achieve source polarizations in excess of 80%.

REFERENCES

1. The result given here supersedes the result presented at Dallas on 8-7-92. The new number is the result of improved statistics and the correction of an overall sign error in the Compton polarimeter analysis.
2. We define the parameter $\sin^2 \theta_W^{\text{lept}}$ in terms of the ratio of vector and axial vector coupling strengths of the Z to the electron, $\sin^2 \theta_W^{\text{lept}} \equiv (1 - v_e/a_e)/4$.
3. Many of the important properties of A_{LR} are discussed in D.C. Kennedy, B.W. Lynn, C.J.-C. Im, and R.G. Stuart *Nuc. Phys.* **B321**, 83 (1989).
4. The product of detector acceptance and efficiency can vary according to decay mode provided the acceptance-efficiency product for each final state is an even function of $\cos \theta$, where θ is the polar angle of the final state fermion with respect to the electron beam direction. This condition is required to cancel terms in the differential cross section that are odd in $\cos \theta$. An even acceptance-efficiency product follows automatically if the efficiency for detecting a fermion at some polar angle θ is equal to the efficiency for detecting an antifermion at the same polar angle. Detectors with axially symmetric solenoidal magnetic fields (e.g. the SLD) have this property.
5. D. Blockus *et al.*, Proposal for Polarization at the SLC, April 1986.
6. The SLC polarized electron gun is described in D. Schultz *et al.*, SLAC-PUB-5768, 1992, and the laser system is described in J. Frisch *et al.*, SLAC-PUB-5965, 1992.
7. J. Kent *et al.*, SLAC-PUB-4922, March 1989.
8. See S.B. Gunst and L.A. Page, *Phys. Rev.* **92**, 970 (1953) or H.A. Olsen, *Applications of QED*, Springer Tracts in Modern Physics, Vol. 44, p.83, (1968).
9. The orientations of the fast and slow axes of the quarter-wave plate were checked by comparing the phase difference induced by the plate with the calculable phase shift induced by total internal reflection in a glass prism.
10. See Reference 7 and G.S. Abrams *et al.*, *Phys. Rev. Lett.*, **63**, 2173 (1989).
11. K. Yokoya and P. Chen, SLAC-PUB-4692, September 1988, and P. Chen private communication.
12. The SLD Design Report, SLAC Report 273, 1984.
13. D. Axen *et al.*, The Lead-Liquid Argon Sampling Calorimeter of the SLD Detector, SLAC-PUB-5354, 1992 (to be published in Nuclear Instruments and Methods).

14. A.C. Benvenuti *et al.*, Invited talk at the 2nd International Conference on Calorimetry in High Energy Physics, Capri, Italy, October 1991, SLAC-PUB-5713.
15. S.C. Berridge *et al.*, Proceedings of the 1991 Nuclear Science Symposium, Santa Fe, NM, vol. 1, page 495; SLAC-PUB-5694 (to be published in IEEE Trans. Nucl. Sci.).
16. D. Muller in these proceedings.
17. We use the theoretical sign of the Compton scattering asymmetry and the measured helicity of the Compton laser to infer the correct sign of the beam helicity.
18. The flux of beamstrahlung photons produced at the IP is related to many of the parameters that determine the luminosity but is not a direct measure of the luminosity.
19. Our own calculation agrees with the results given by the EXPOSTAR program described in D.C. Kennedy *et al.*, *Z. fur Phys.*, **C53**, p.617, 1992, and a modified version of the ZSHAPE program described in CERN 89-08, vol. 3, p. 50, 1989.
20. L. Rolandi in these proceedings.
21. T. Maruyama, *et al.*, *Phys. Rev. B*, **46**, 4261 (1992).

LIST OF AUTHORS

K. Abe,²⁰ I. Abt,²⁸ P. D. Acton,³ G. Agnew,³ C. Alber,²⁶ D. F. Alzofon,¹⁹ P. Antilogus,¹⁹ C. Arroyo,⁵ W. W. Ash,¹⁹ V. Ashford,¹⁹ A. Astbury,³² D. Aston,¹⁹ Y. Au,⁵ D. A. Axen,²⁴ N. Bacchetta,⁹ K. G. Baird,¹⁷ W. Baker,¹⁹ C. Baltay,³⁶ H. R. Band,³⁴ G. J. Baranko,²⁶ O. Bardou,¹⁵ F. Barrera,¹⁹ R. Battiston,¹⁰ D. A. Bauer,²² A. O. Bazarko,⁵ A. Bean,²² G. Beer,³² R. J. Belcinski,²⁹ R. A. Bell,¹⁹ R. Ben-David,³⁶ A. C. Benvenuti,⁷ R. Berger,¹⁹ S. C. Berridge,³¹ S. Bethke,¹⁴ M. Biasini,¹⁰ T. Bienz,¹⁹ G. M. Bilei,¹⁰ F. Bird,¹⁹ D. Bisello,⁹ G. Blaylock,²³ R. Blumberg,¹⁹ J. R. Bogart,¹⁹ T. Bolton,⁵ S. Bougerolle,²⁴ G. R. Bowler,¹⁹ R. F. Boyce,¹⁹ J. Brau,³⁰ M. Breidenbach,¹⁹ T. E. Browder,¹⁹ W. M. Bugg,³¹ B. Burgess,¹⁹ D. Burke,¹⁹ T. H. Burnett,³³ P. N. Burrows,¹⁵ W. Busza,¹⁵ B. L. Byers,¹⁹ A. Calcaterra,¹² D. O. Caldwell,²² D. Calloway,¹⁹ B. Camanzi,⁸ L. Camilleri,⁵ M. Carpinelli,¹¹ J. Carr,²⁶ S. Cartwright,²⁹ R. Cassell,¹⁹ R. Castaldi,¹¹ ²⁷ A. Castro,⁹ M. Cavalli-Sforza,²³ G. B. Chadwick,¹⁹ O. Chamberlain,¹⁴ D. Chambers,¹⁹ L. Chen,³⁵ P.E.L. Clarke,³ R. Claus,¹⁹ J. Clendenin,¹⁹ H. O. Cohn,³¹ J. A. Coller,² V. Cook,³³ D. Cords,¹⁹ R. Cotton,³ R. F. Cowan,¹⁵ P. A. Coyle,²³ D. G. Coyne,²³ W. Craddock,¹⁹ H. Cutler,¹⁹ A. D'Oliveira,²⁵ C.J.S. Damerell,¹⁸ S. Dasu,¹⁹ R. Davis,¹⁹ R. De Sangro,¹² P. De Simone,¹² S. De Simone,¹² T. Dean,¹⁹ F. Dejongh,⁴ R. Dell'Orso,¹¹ A. Disco,³⁶ R. Dolin,²² R. W. Downing,²⁸ Y. C. Du,³¹

R. Dubois,¹⁹ J. E. Duboscq,²² W. Dunwoodie,¹⁹
D. D. Durrett,²⁶ G. Eigen,⁴ B. I. Eisenstein,²⁸
R. D. Elia,¹⁹ W. T. Emmet, II,³⁶ R. L. English,¹⁸
E. Erdos,²⁶ J. Escalera,¹⁹ C. Fan,²⁶ M. J. Fero,¹⁵
J. Ferrie,¹⁹ T. Fieguth,¹⁹ J. Flynn,¹⁹ D. A. Forbush,³³
K. M. Fortune,²⁸ J. D. Fox,¹⁹ M. J. Fox,¹⁹
R. Frey,³⁰ D. R. Freytag,¹⁹ J. I. Friedman,¹⁵
J. Fujimoto,¹³ K. Furuno,³⁰ M. Gaillard,¹⁹
M. Gallinaro,¹² E. Garwin,¹⁹ T. Gillman,¹⁸
A. Gioumousis,¹⁹ G. Gladding,²⁸ S. Gonzalez,¹⁵
D. P. Gurd,²¹ D. L. Hale,²² G. M. Haller,¹⁹
G. D. Hallewell,¹⁹ V. Hamilton,¹⁹ M. J. Haney,²⁸
T. Hansl-Kozanecka,¹⁵ H. Hargis,³¹ J. Harrison,³³
E. L. Hart,³¹ K. Hasegawa,²⁰ Y. Hasegawa,²⁰
S. Hedges,³ S. S. Hertzbach,²⁹ M. D. Hildreth,¹⁹
R. C. Hilomen,¹⁹ D. G. Hitlin,⁴ T. A. Hodges,³²
J. Hodgson,¹⁹ J. J. Hoeflich,¹⁹ A. Honma,³²
D. Horelick,¹⁹ J. Huber,³⁰ M. E. Huffer,¹⁹ E. W.
Hughes,¹⁹ H. Hwang,³⁰ E. Hyatt,⁵ Y. Iwasaki,²⁰
J. M. Izen,²⁸ P. Jacques,¹⁷ C. Jako,¹⁹ A. S. Johnson,²
J. R. Johnson,³⁴ R. A. Johnson,²⁵ S. Jones,¹⁹
T. Junk,¹⁹ S. Kaiser,¹⁹ R. Kajikawa,¹⁶ M. Kalelkar,¹⁷
H. Kang,¹⁹ I. Karliner,²⁸ H. Kawahara,¹⁹ R. K.
Keeler,³² M. H. Kelsey,⁴ H. W. Kendall,¹⁵
D. Kharakh,¹⁹ H. Y. Kim,³³ P. C. Kim,¹⁹
R. King,¹⁹ M. Klein,⁴ R. R. Kofler,²⁹ M. Kowitz,¹⁴
N. M. Krishna,²⁶ R. S. Kroeger,³¹ P. F. Kunz,¹⁹
Y. Kwon,¹⁹ J. F. Labs,¹⁹ R. R. Langstaff,³²
M. Langston,³⁰ R. Larsen,¹⁹ A. Lath,¹⁵ J. A. Lauber,²⁶
D. W. G. Leith,¹⁹ L. Lintern,¹⁸ X. Liu,²³ M. Loreti,⁹
A. Lu,²² H. L. Lynch,¹⁹ T. Lyons,¹⁵ J. Ma,³³
W. A. Majid,²⁸ G. Mancinelli,¹⁰ S. Manly,³⁶
D. Mansour,¹⁹ G. Mantovani,¹⁰ T. W. Markiewicz,¹⁹
T. Maruyama,¹⁹ G. R. Mason,³² H. Masuda,¹⁹
L. Mathys,²² G. Mazaheri,¹⁹ A. Mazzucato,⁹
E. Mazzucato,⁸ J. F. McGowan,²⁸ S. McHugh,²²
A. K. McKemey,³ B. T. Meadows,²⁵ D. J. Mellor,²⁸
R. Messner,¹⁹ A. I. Mincer,⁴ P. M. Mockett,³³
K. C. Moffeit,¹⁹ R. J. Morrison,²² B. Mours,¹⁹
G. Mueller,¹⁹ D. Muller,¹⁹ G. Mundy,¹⁹ T. Nagami-
mine,¹⁹ U. Nauenberg,²⁶ H. Neal,¹⁹ D. Nelson,¹⁹
V. Nesterov,¹⁹ M. Nordby,¹⁹ M. Nussbaum,²⁵
A. Nuttall,¹⁹ H. Ogren,⁶ J. Olsen,¹⁹ C. Oram,²¹
L. S. Osborne,¹⁵ R. Ossa,¹⁹ G. Oxoby,¹⁹ L. Paffrath,¹⁹
A. Palounek,¹⁵ R. S. Panvini,³⁵ H. Park,³⁰
M. Pauluzzi,¹⁰ T. J. Pavel,¹⁹ F. Perrier,¹⁹ I. Peruzzi,¹²
10. L. Pescara,⁹ D. Peters,²⁴ H. Petersen,¹⁹
M. Petradza,¹⁹ M. Piccolo,¹² L. Piemontese,⁸
E. Pieroni,¹¹ R. Pitthan,¹⁹ K. T. Pitts,³⁰
R. J. Plano,¹⁷ P. R. Poffenberger,³² R. Prepost,³⁴
C. Y. Prescott,¹⁹ D. Pripstein,¹⁴ G. D. Punkar,¹⁹
G. Putallaz,¹⁹ P. Rankin,²⁶ B. N. Ratcliff,¹⁹
T. W. Reeves,³⁵ P. E. Rensing,¹⁹ J. D. Richman,²²
R. Rinta,¹⁹ L. P. Robertson,³² L. S. Rochester,¹⁹
L. Rosenson,¹⁵ J. E. Rothberg,³³ A. Rothenberg,¹⁹
P. C. Rowson,⁵ J. J. Russell,¹⁹ D. Rust,⁶
E. Rutz,²⁵ P. Saez,¹⁹ B. Saitta,⁸ A. K. Santha,²⁵

A. Santocchia,¹⁰ O. H. Saxton,¹⁹ T. Schalk,²³
P. R. Schenk,³² R. H. Schindler,¹⁹ U. Schneekloth,¹⁵
M. Schneider,²³ D. Schultz,¹⁹ G. E. Schultz,²⁶
B. Schumm,¹⁴ A. Seiden,²³ L. Servoli,¹⁰
M. H. Shaevitz,⁵ J. T. Shank,² G. Shapiro,¹⁴
S. L. Shapiro,¹⁹ H. Shaw,¹⁹ D. J. Sherden,¹⁹
T. Shimomura,¹⁹ A. Shoup,²⁵ R. L. Shypit,²⁴
C. Simopoulos,¹⁹ K. Skarpaas,¹⁹ S. R. Smith,¹⁹
A. Snyder,¹⁹ J. A. Snyder,³⁶ R. Sobie,²⁴
M. D. Sokoloff,²⁵ E. N. Spencer,²³ S. St. Lorant,¹⁹
P. Stamer,¹⁷ H. Steiner,¹⁴ R. Steiner,¹
R. J. Stephenson,¹⁸ G. Stewart,²⁸ P. Stiles,¹⁹
I. E. Stockdale,²⁵ M. G. Strauss,²⁹ D. Su,¹⁸
F. Suekane,²⁰ A. Sugiyama,¹⁶ S. Suzuki,¹⁶
M. Swartz,¹⁹ A. Szumilo,³³ M. Z. Tahar,²
T. Takahashi,¹⁹ G. J. Tappern,¹⁸ G. Tarnopolsky,¹⁹
F. E. Taylor,¹⁵ M. Tecchio,⁹ J. J. Thaler,³⁶
F. Toevs,³³ N. Toge,¹⁹ M. Turcotte,³² J. D. Turk,³⁶
T. Usher,¹⁹ J. Va'Vra,¹⁹ C. Vannini,¹¹ E. Vella,³³
J. P. Venuti,³⁵ R. Verdier,¹⁵ P. G. Verdini,¹¹
B. F. Wadsworth,¹⁵ A. P. Waite,¹⁹ D. Walz,¹⁹
D. Warner,² R. Watt,¹⁹ S. J. Watts,³ T. Weber,¹⁹
A. W. Weidemann,³¹ J. S. Whitaker,² S. L. White,³¹
F. J. Wickens,¹⁸ S. A. Wickert,²² D. A. Williams,²³
D. C. Williams,¹⁵ R. W. Williams,³³ S. H. Williams,¹⁹
R. J. Wilson,² W. J. Wisniewski,⁴ M. S. Witherell,²²
M. Woods,¹⁹ G. B. Word,¹⁷ J. Wyss,⁹
R. K. Yamamoto,¹⁵ J. M. Yamartino,¹⁵ C. Yee,¹⁹
S. J. Yellin,²² A. Yim,¹⁹ C. C. Young,¹⁹
K. K. Young,³³ H. Yuta,²⁰ G. Zapalac,³⁴
R. W. Zdarko,¹⁹ C. Zeitlin,³⁰ M. Zolotorev,¹⁴
and P. Zuchelli,⁸

LIST OF INSTITUTIONS

¹ Adelphi University, ² Boston University, ³ Brunel University, ⁴ California Institute of Technology, ⁵ Columbia University, ⁶ Indiana University, ⁷ INFN Sezione di Bologna, ⁸ INFN Sezione di Ferrara and Università di Ferrara, ⁹ INFN Sezione di Padova and Università di Padova, ¹⁰ INFN Sezione di Perugia and Università Perugia, ¹¹ INFN Sezione di Pisa and Università di Pisa, ¹² INFN Lab. Nazionali di Frascati, ¹³ KEK National Laboratory, ¹⁴ Lawrence Berkeley Laboratory, University of California, ¹⁵ Massachusetts Institute of Technology, ¹⁶ Nagoya University, ¹⁷ Rutgers University, ¹⁸ Rutherford Appleton Laboratory, ¹⁹ Stanford Linear Accelerator Center, ²⁰ Tohoku University, ²¹ TRIUMF ²² University of California, Santa Barbara, ²³ University of California, Santa Cruz, ²⁴ University of Cincinnati, ²⁶ University of Colorado, ²⁷ Università di Genova, ²⁸ University of Illinois, ²⁹ University of Massachusetts, ³⁰ University of Oregon, ³¹ University of Tennessee, ³² University of Victoria, TRIUMF, ³³ University of Washington, ³⁴ University of Wisconsin, ³⁵ Vanderbilt University, ³⁶ Yale University.